Separation of Pulse Tube Losses Based on Measurement of Energy Flow and Computational Fluid Dynamics Analysis

T. Ki and S. Jeong

Cryogenic Engineering Laboratory
Korea Advanced Institute of Science and Technology, Korea

ABSTRACT

Pulse tube losses in pulse tube refrigerator consist of shuttle heat transfer loss, second-order flow loss, and natural convection loss. It is difficult to quantify the pulse tube losses in the actual operating condition. In this paper, the pulse tube losses are precisely measured and separated by the measurement of energy flow and Computational Fluid Dynamics (CFD) analysis. First, a Stirling-type pulse tube refrigerator is fabricated. The detailed physical conditions of the working fluid are measured at each critical component of Stirling-type pulse tube refrigerator. The summation of the pulse tube losses is calculated by the energy flow concept and the measured results. Second, the physical conditions of the measured results are used in the CFD analysis to separate the pulse tube losses. In this process, the separation of pulse tube losses is confirmed and the portion of each pulse tube loss is evaluated. The results of this paper can be used to better understand the tendency of pulse tube losses and can confirm the accuracy of the equations proposed to estimate each loss generated in a pulse tube.

INTRODUCTION

To improve the performance of pulse tube refrigerator (PTR), the generated losses need to be identified and effectively reduced. The pulse tube losses generated in a pulse tube consist of shuttle heat transfer loss, second-order flow loss, and natural convection loss. The shuttle heat transfer loss is generated from the heat transfer process between the pulse tube wall and the oscillating gas having the different temperature profiles. Since the oscillating gas near the side wall in a pulse tube experiences different viscosity changes during the positive and the negative flows, the net mass flow rate near the wall moves toward the warm-end of pulse tube. The process generates circulating flow and the heat is transferred from the warm side to the cold side in a pulse tube. This loss is called the second-order flow loss. The cause for natural convection loss is natural convection generated due to gravity. The pulse tube losses greatly influence the performance of PTR. It is important to quantify and estimate the pulse tube losses to seek a reduction in these losses. Much research has been performed based on numerical simulation to identify the pulse tube losses. The simulation is a good tool to simply confirm the tendency, but the accuracy of simulation is very dependent on the assumptions and the skill. For accurate design and PTR performance estimation, the precise measurement of losses generated in a pulse tube is necessary and the experimental measurement should be used to revise the simulation results.

Cryocoolers 17, edited by S.D. Miller and R.G. Ross, Jr.

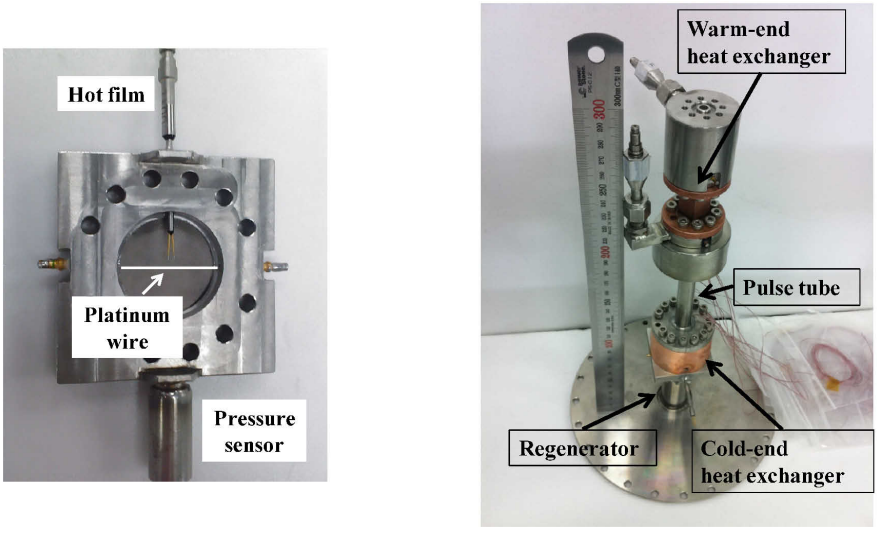

(a) (b)

Figure 1. (a) Developed instrumentation for real-time measurement. (b) PTR combined with instrumentation.

In this paper, the quantification and the separation of pulse tube losses, i.e. the shuttle heat transfer loss and the second-order flow loss, are carried out through the measurement of energy flow and CFD analysis. In our past work[1] presented at CEC/ICMC 2011, the detailed physical conditions of the working fluid were carefully measured for each component of the Stirling-type PTR from real-time measurement techniques and the summation of pulse tube losses was obtained. The measured boundary conditions of pulse tube are used in CFD analysis to separate the pulse tube losses. A CFD model for the pulse tube is set up, and thermal and fluid dynamics in the pulse tube are investigated for the cyclic steady state. In this process, the separation concept is proposed and the quantities of each loss in the pulse tube are obtained by using CFD analysis and the proposed separation concept.

ENERGY FLOW MEASUREMENT

In our past work[1], physical conditions such as mass flow rate, pressure, and temperature were measured for the energy analysis. The wall surface temperatures were measured by 14 E-type thermocouples installed along the wall of the pulse tube to be compared with the CFD analysis results. Figure 1 shows the instrumentation developed to measure the cross-sectional parameters and the PTR combined with the instrumentation. Figure 2 shows the measured mass flow rate and the temperature curves at the cold end of regenerator. All measured physical conditions were transformed into the cosine and sine series of Fourier function and the enthalpy, the PV work, and the entropy flows were calculated by the following equations.

$$\left\langle \dot{H}_{REG} \right\rangle = \frac{1}{\tau}\int_0^{\tau} C_P \dot{m} T dt \tag{1}$$

where $< \dot{H}_{REG} >$ is the cycle average regenerator enthalpy flow generated from the ineffectiveness of the regenerator, C_P is the specific heat, T is the gas temperature, $\dot{m}$ is the mass flow rate, and τ is the period.

$$\left\langle \dot{H}_{PT} \right\rangle = \left\langle P\dot{V} \right\rangle + T\left\langle \dot{S} \right\rangle \tag{2}$$

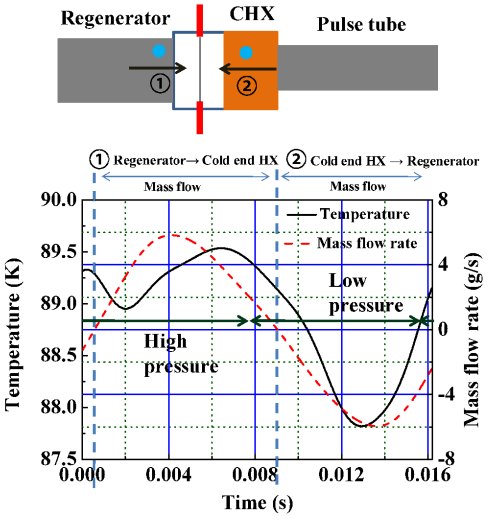

Figure 2. Measured temperature and mass flow rate curves at 60 Hz.

$$\left\langle P\dot{V}\right\rangle = \frac{1}{\tau}\int_0^{\tau} P\dot{V}dt \tag{3}$$

where $< \dot{H}_{PT} >$ is the cycle average pulse tube enthalpy flow, $< P\dot{V} >$ is the cycle average PV work flow, $< \dot{S} >$ is the cycle average entropy flow, P is the pressure, and $\dot{V}$ is the volume flow rate. Here, the entropy flow ($T< \dot{S} >$) is composed of the quantity generated from the pulse tube loss. The pulse tube losses are composed of the shuttle heat transfer loss, the second-order flow loss, and the natural convection loss. After the quantity ($T< \dot{S} >$) of pulse tube losses is obtained from the analysis of energy flow represents the summation of the losses, i.e. the shuttle heat transfer loss, the second-order flow loss, and the natural convection loss, each loss should be separated for detailed quantification. Table 1 presents the calculated enthalpy, PV work, and entropy flows in the PTR.

CFD ANALYSIS AND SEPARATION CONCEPT

In our experimental condition, the natural convection loss can be neglected because the cold end of the pulse tube is positioned lower than the hot end of pulse tube and the operating frequency is high. When the gas in the pulse tube is set as the control volume as shown in Figure 3, the transferred heat is considered a part of the cycle average heat flux (Q_1) transferred from the inner wall of pulse tube and the cycle average heat fluxes (Q_2) transferred from the boundary of warm side to the boundary of cold side. The quantity of shuttle heat transfer loss is included in the quantity calculated from the cycle average heat flux between the inner wall and the gas; because the sources of shuttle heat transfer loss is the interaction between the shuttle gas and the wall. The cycle average heat flux transferred between the inner wall of pulse tube and the gas also includes the quantity of loss generated by the second-order flow.

The average heat flux (q''_s) of the total surface of the inner wall generated from the shuttle heat transfer process can be expressed by a Fourier series.

$$q''_s = A + B\sin(\omega t + \theta_1) + C\cos(\omega t + \theta_2) \tag{4}$$

where ω is angular frequency, t is time, and θ is phase. The quantity has steady and oscillating terms because the oscillating gas generates the net and the oscillating heat fluxes

Table 1. Enthalpy flow, work flow, and various losses in PTR.

Frequency	60 Hz		58 Hz		55 Hz	
Charging pressure	2.5 MPa					
Pressure ratio	1.2		1.18		1.16	
Mechanical work (Piston stroke)	251.5 W (4.51 mm)		216.6 W (4.06 mm)		155.5 W (3.42 mm)	
PV work in hot-end of regenerator	203 W		175.5 W		127 W	
Enthalpy flow in regenerator	Hot-end	9.5 W	Hot-end	8.2 W	Hot-end	5.9 W
	Cold-end	9.9 W	Cold-end	8.8 W	Cold-end	7.1 W
PV work flow in cold-end of pulse tube	42.2 W		37.6 W		28.2 W	
Cooling capacity	17.7 W		14.7 W		8.6 W	
Pressure drop loss of regenerator	21 W		17.7 W		13.1 W	
Pulse tube losses	12.6 W		12 W		10.5 W	
Enthalpy flow in pulse tube	29.6 W		25.6 W		17.7 W	
Conduction loss	1.98 W		2.1 W		2.04 W	

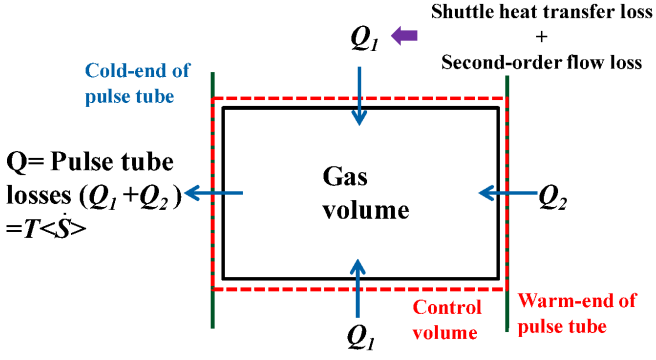

Figure 3. Heat transferred in control volume of pulse tube.

between the wall and the gas. The quantity of the shuttle heat transfer loss is the cycle average heat flux (A) multiplied by the inner wall surface area of the pulse tube.

The average heat flux (q''_{2nd}) of the inner total wall surface generated from the circulating second-order flow can be expressed by Eq. (5).

$$q''_{2nd} = D \tag{5}$$

The average heat flux of the inner wall total surface related to second-order flow loss will have only steady terms because the gas flow generated from the second-order flow is inherently steady near the inner wall. Therefore, the average total heat flux of inner wall total surface is:

$$q'' = A + D + B\sin(\omega t + \theta_1) + C\cos(\omega t + \theta_2) \tag{6}$$

It is difficult to perfectly decouple the part (A) of shuttle gas from the steady terms (A+D) of total heat flux. However, if the relation between the mass flow rate of the shuttle gas and the average total heat flux is known, the decoupling process is possible. Figure 4 shows the mechanism of the shuttle heat transfer loss[2]. The net heat is transferred to the cold-end part by the displacer and the shuttle gas. The relation between the mass flow rate curve averaged along a pulse tube and the total heat flux curve of shuttle gas averaged along an inner wall of pulse tube is shown in Figure 4(b). When the relation between the motion of the shuttle gas and the heat transferred to the shuttle gas are considered like the relation between the motion of displacer and the heat transferred to the displacer as shown in Fig. 4(a), the mass flow rate curve averaged along a pulse tube is approximately leading the total heat flux curve averaged along an inner wall of pulse tube by 90 degree. We realize that when the position of shuttle gas is located at the neutral position (②, ④): the heat flux is zero. Therefore, the heat flux is zero in the maximum and the minimum points of the mass flow rate curve. However, the heat flux is not actually zero at the points because the second-order flow loss exists. The heat flux curve is shifted by the quantity (D) of the second-order flow loss. The quantity of heat flux in the maximum and the minimum points of mass flow rate curve mean the quantity of heat flux generated from the second-order flow loss. If the average total heat flux and mass flow rate curves in a pulse tube are known, each average heat flux (A, D) generated from the shuttle gas and the second-order flow will be separated from the average total heat flux (q''). The subtracting the heat loss calculated from the average total heat flux from the summation of pulse tube losses gives the quantity that is the heat loss transferred from the warm-side boundary of pulse tube. The separation of pulse tube losses can be possible by using this method.

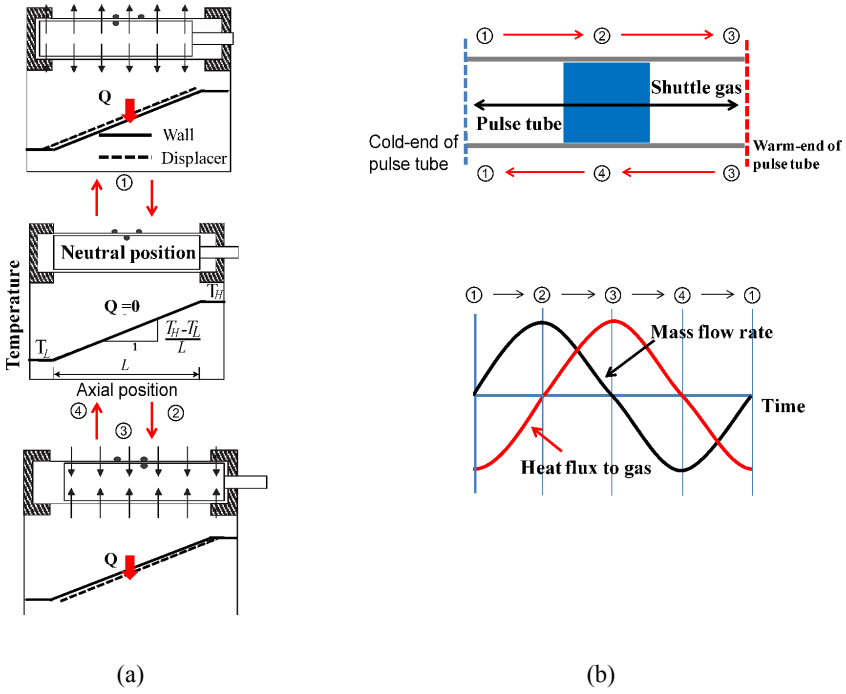

(a) (b)

Figure 4. (a) Mechanism[2] of shuttle heat transfer loss in Stirling cryocooler. (b) Estimated relation between average mass flow rate and average total heat flux curves of gas piston in pulse tube.

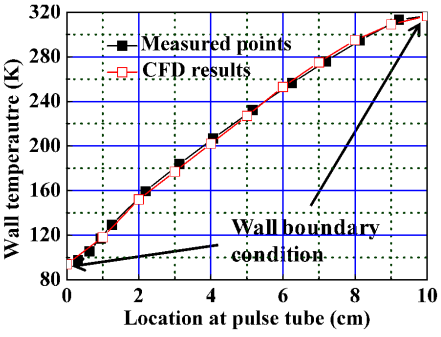

Figure 5. Comparison of measured and calculated surface temperatures.

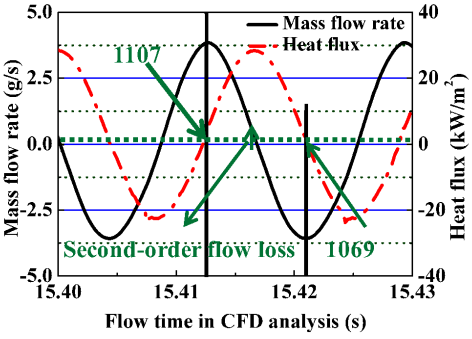

Figure 6. Heat flux and mass flow rate curves averaged along pulse tube.

The average heat flux and average mass flow rate curves in a pulse tube can be obtained from the CFD results. In order to confirm the use of the proposed method, the CFD modeling is compared to our past experiment result. FLUENT is used for the CFD modeling of the pulse tube. In GAMBIT, the 2D configuration (wall and inner space of the pulse tube) of the fabricated pulse tube is described and the meshing process is carefully executed. In oscillating flow condition of the pulse tube, the flow regime is determined by the flow map presented from Brereton et. al.[3] On the basis of the measured physical condition, the flow regime of the pulse tube is in the perturbed laminar range. The laminar model of FLUENT is used, and PISO and the second-order upwind scheme are used. The pressure and the mass flow rate measured by the experiment are used to define the realistic boundary conditions of both sides of the pulse tube, and the outside area of the wall is set as the adiabatic condition. The accuracy of the results calculated by the CFD process can be verified by comparing the calculated and the measured wall temperatures of the pulse tube.

CFD AND SEPARATION RESULTS

In this paper, the case of 60 Hz in Table 1 is used for the CFD analysis. When the wall temperatures of the pulse tube calculated by the CFD are not changed, the calculation results are considered to reach the cyclic steady state condition. Figure 5 shows the surface temperatures of the wall measured in our past experiment and calculated by the CFD analysis. Since the measured and the calculated surface temperatures are very close, the results calculated by the developed CFD analysis are credible. Figure 6 shows the average total heat flux curve of gas along the inner wall surface and the average mass flow rate curve along the pulse tube. The average total heat flux curve is expressed as follows:

$$q'' = 2958 + 18360\cos(376.9t) - 17520\sin(376.9t) \quad (\mathrm{W/m^2}) \tag{7}$$

The steady term (2958 W/m^2) is the net heat flux transferred from the wall of pulse tube to the shuttle gas and the second-order flow in the cyclic steady state condition. The quantity (Q_1 in Fig. 3) of heat loss is 11.15 W (0.00377 (surface area of pulse tube) x 2958). Since the measured total pulse tube losses is 12.6 W, the heat loss (Q_2 in Fig. 3) transferred from the warm-side boundary of pulse tube is 1.45 W. In the average total heat flux curve, the average quantity of heat flux is 1088 W/m^2 ((1107+1069)/2) at the maximum and the minimum points of average mass flow rate curve as shown in Fig. 6. Therefore, the quantity of second-order flow loss is 4.1 W and the quantity of shuttle heat transfer loss is 7.05 W. Table 2 presents the result obtained from the proposed separation method.

Table 2. Separation result of pulse tube losses.

Summation of Pulse tube losses	Cycle average total heat flux transferred from wall	Shuttle heat transfer loss	Second-order flow loss	Heat loss transferred from warm-side boundary of pulse tube
12.6 W	**2958 W/m^2**	**7.05 W**	**4.1 W**	**1.45 W**

DISCUSSION

In Table 3, each quantity of the separated pulse tube losses is compared to the quantities calculated by the proposed equations in the references[4-6]. The physical conditions measured in our past work are used in the proposed equations to obtain the shuttle heat transfer loss and the second-order flow loss. The differences between the losses calculated from the references and the losses obtained from the proposed separation process and the real-time measurement in this paper are large. The references present the importance of each loss generated in a pulse tube and qualitatively show the tendency of each loss, but the exactly calculated quantities of losses in this paper have a significant difference. The reason may be attributed to the assumptions of references. We think the quantity of each loss obtained from this paper is more accurate than those calculated from the references [4-6], because the quantities of each loss proposed in this paper are obtained from experimental measurement and the analysis from the verified CFD model. If new or updated equations estimating the quantity of each loss of pulse tube are proposed, the accuracy of the equations can be better judged by the quantity of each loss obtained from this paper.

CONCLUSION

In this paper, the pulse tube losses are separated by a real-time measurement and a CFD analysis. The detailed physical conditions of working fluid are measured at each critical component in a fabricated PTR. By using the measured physical conditions, we know how the energy is transferred. In this process, the losses generated in the fabricated PTR are exactly quantified and the pulse tube losses (shuttle heat transfer and second-order flow losses) are obtained as the combined quantity. To separate the combined pulse tube losses, a separating concept using CFD analysis is proposed. A CFD model is developed for separation of pulse tube losses and the measured physical conditions are used for the boundary conditions of CFD model. The accuracy of results obtained from the developed CFD is confirmed by comparison with the

Table 3. Comparison of each pulse tube loss with references.

	Shuttle heat transfer loss	Second-order flow loss
This paper	**7.05 W**	**4.1 W**
Reference [4]	**33.4 W** (63 W (Enthalpy flow at the adiabatic pulse tube obtained from expansion efficiency) - 29.6 W (Enthalpy flow obtained in our past experiment)), Expansion efficiency = 0.47 (29.6/Enthalpy flow at the adiabatic pulse tube), Calculated condition = β_w : 40.2, r_T : 90/317, R_P : 0.092, Re[$U_{amp,w}/\omega V_{PT}$] : -0.1454	-
Reference [5,6]	**1.45 W** (Mean Valensi number : 6684, Mean tidal amplitude/length of pulse tube = 0.1256)	**0.4 W**

measured surface temperatures of wall. By using the proposed separation concept, the quantity of pulse tube losses (12.6 W) is finally separated into the shuttle heat transfer loss (7.05 W), the second-order flow loss (4.1 W), and a heat loss transferred from the warm-side boundary of pulse tube (1.45 W). If new or updated equations estimating the quantity of each loss of pulse tube are proposed, the accuracy of the equations can be confirmed by the results in this paper.

ACKNOWLEDGMENT

This research was supported by the Converging Research Center Program funded by the Ministry of Education, Science and Technology (No. 2011K000778).

REFERENCES

1. Ki, T., Jeong, S., Seo, M., and Park, I., “Measurement and analysis of energy flow Stirling-type pulse tube refrigerator,” *Adv. in Cryogenic Engineering*, Vol. 57, Amer. Institute of Physics, Melville, NY (2012), pp. 555-562.
2. Chang, H. M., Park, D. J., and Jeong, S., "Effect of gap flow on shuttle heat transfer," *Cryogenics*, Vol. 40, Issue: 3 (March 2000), pp. 159-166.
3. Brereton, G. J., and Mankbadi, R. R., “Review of recent advances in the study of unsteady turbulent internal flows," *Appl. Mech. Rev.*, Vol. 48, Issue: 4 (April 1995), pp. 189-212.
4. Jung, J., and Jeong, S., "Expansion efficiency of pulse tube in pulse tube refrigerator including shuttle heat transfer effect," *Cryogenics*, Vol. 45, Issue: 5 (May 2005), pp. 386-396.
5. Olson, J. R., and Swift, G. W., "Acoustic streaming in pulse tube refrigerator : tapered pulse tubes," *Cryogenics*, Vol. 37, Issue: 12 (December 1997), pp. 769-776.
6. Gedeon, D., *SAGE® Stirling cycle model class reference guide*, Gedeon Associates, Athens, OH, USA, April 2006, pp. 155-156.